Progress In Electromagnetics Research Letters, Vol. 59, 93–99, 2016

Ka-band Radiation Pattern Reconfigurable Antenna Based on Microstrip MEMS Switches

Zhongliang Deng, Jun Gan*, Hao Wei, Hua Gong, and Xubing Guo

Abstract—This paper presents the use of micro-electromechanical systems (MEMS) switches to realize the radiation pattern reconfiguration of microstrip antenna, which works in Ka-band. The antenna was fabricated on a silicon substrate and designed to reconfigure radiation pattern at the operation frequency of 35 GHz. The simulation results show that by controlling the states of MEMS switches between the driven element and two parasitic elements, the antenna can achieve reconfiguring into three maximum radiation directions in the H-plane ($\theta = 0°$, $\psi = 90°$, $\theta = 14°$, $\psi = 90°$, and $\theta = -14°$, $\psi = 90°$, respectively). The measured maximum radiation directions of modes-1, modes-2, modes-3, modes-4 are $\theta = 17°$, $-25.8°$, $3.5°$, $0.7°$ and gains of four modes at the maximum radiation direction are 5.78 dBi, 6.49 dBi, 7.24 dBi, 6.31 dBi, respectively. The measured results are closely consistent with the simulation ones. The proposed antenna can be applied to satellite communication.

1. INTRODUCTION

Reconfigurable antennas have drawn a lot of attention in the wireless communication systems for their multifunctions and additions of freedom degrees. They can dynamically alter their radiation characteristics such as frequency, polarization, radiation pattern, etc. by changing its electrical or physical configuration [1–3]. In this manner, multiple functions can be integrated on a single antenna, resulting in considerable saving in cost and size. Because changing operating frequency while maintaining radiation patterns and polarization could make antenna work in different band. If the antenna could change radiation pattern, but maintaining operating frequency and bandwidth, the system performance will be greatly enhanced. Manipulation of an antenna's radiation pattern can be used to avoid noise of sources, improve efficiency by directing signals only toward intended users. Polarization diversity is used to avoid the detrimental fading loss caused by multipath effect. Many microstrip reconfigurable antennas have been proposed in the past that use pin diodes [4], copper strip [5] or MEMS switches [6, 7]. However, compared with conventional semiconductor-based passive devices, MEMS technology enables the realization of RF passive components with low loss, high isolation, small size, low power consumption, high quality factors, high tunable characteristics and high linearity. So in recent year, MEMS switches are used broadly in reconfigurable antennas [8–10], but most of which work in low frequency. Compared with low frequency antennas, millimeter band antennas have several advantages. First, antennas can be more directive with the same aperture size. Second, it greatly reduces the size of the antenna, which is more suitable for the combination with MEMS devices. Finally, Ka-band antenna, compared to C-band and Ku-band, provides more powerful data throughput, which can be applied to satellite communication [11].

In this paper, a radiation pattern reconfigurable patch antenna, based on MEMS switches and works in Ka band, is presented. It consists of one driven patch, two parasitic patches and two MEMS switches. By changing the states of the MEMS switches, the surface current distribution is affected,

Received 12 January 2016, Accepted 21 March 2016, Scheduled 6 April 2016

* Corresponding author: Jun Gan (GanJ@bupt.edu.cn).

The authors are with the School of Electronic Engineering, Beijing University of Posts and Telecommunications, Beijing 100876, China.

which leads to reconfiguration of the radiation pattern. The antenna can achieve reconfiguration into two modes in the H-plane ($\theta = 14°$, $\psi = 90°$, and $\theta = 14°$, $\psi = 90°$, respectively) at the maximum beam directions. The measured maximum radiation directions of modes-1, modes-2, modes-3, modes-4 are $\theta = 17°$, $-25.8°$, $3.5°$, $0.7°$ and gains of four modes at the maximum radiation direction are 5.78 dBi, 6.49 dBi, 7.24 dBi, 6.31 dBi, respectively. Detailed structures and simulated performance of MEMS switches are presented in [12]. The paper mainly analyzes pattern reconfigurable principles and gives the compare between simulated results and measured results.

2. PHYSICAL STRUCTURE AND RADIATION MECHANISM

2.1. Microstrip Patch and MEMS Switch Design

As illustrated in Fig. 1, the proposed antenna consists of two MEMS switches and three microstrip patches, which includes one driven element and two parasitic elements. Fig. 1 shows the geometry of the proposed reconfigurable antenna and microstrip MEMS switch. The antenna is designed on high resistivity silicon which is 0.4 mm thick with relative dielectric constant, $\varepsilon_r = 11.9$. The main dimensions of the antenna are listed in Table 1. The dimensions of the driven element are 1.5 mm × 0.9 mm. The driven patch width W_0 is approximately half of the guided wavelength at the resonant frequency of 35 GHz, and the parasitic elements are 0.96 mm × 0.97 mm, which is smaller than the driven patch. The gap between any two patches is 0.6 mm. The feed point of a 50 Ω microstrip feeding line g lies in antenna center.

As show in Fig. 1(a) and Fig. 1(b) the proposed antenna uses microstrip MEMS switches to realize the radiation reconfiguration. In the coplanar waveguide (CPW) structure, MEMS shunt switches are connected directly to the ground plane through anchor. However, if MEMS switches are employed in the microstrip circuit, the anchor must be connected to the ground plane through vias or $\lambda_g/4$ open stub. But the vias will introduce series inductance and resistance which will have a great impact on the resonant frequency and return loss of the antenna [13]. So this paper uses microstrip MEMS switch with $\lambda_g/4$ open stub to connect with the ground plane. The open stub is one sector of $\alpha = 23°$. By varying the air gap between MEMS switch beam and the signal lines, it can make the switch work in different states. Fig. 1(c) and Fig. 1(d) show two states of MEMS switch, when the air gap is 0.15 μm, capacitance between the signal line and beam is large enough, which leads to the most of current signal coupling to the open stub, the switch is in the down state. But when air gap is 2 μm. The switch is in the up state, and most of the current signals can flow from the drive patch to parasitic patch.

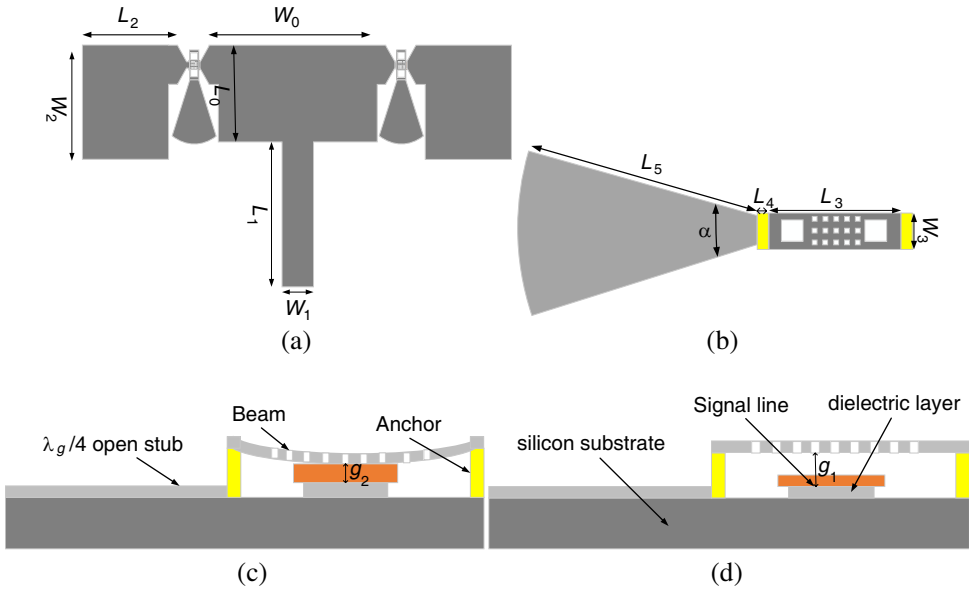

Figure 1. Top view of proposed (a) reconfigurable antenna and (b) microstrip MEMS switch, side view of MEMS switch in (c) down state and (d) up state.

Table 1. Detail dimensions of the antenna.

Symbol	Quantity	Dimension
H	Substrate Thick	0.4 mm
T_0	Patch Thick	2 μm
T_1	Beam Thick	1.5 μm
L_0	Driven Patch Length	0.9 mm
W_0	Driven Patch Wide	1.5 mm
L_1	Feed Length	1.41 mm
W_1	Feed Wide	0.11 mm
L_2	Parasitic Patch Length	0.96 mm
W_2	Parasitic Patch Length	0.97 mm
L_3	Beam Length	280 μm
W_3	Beam Wide	90 μm
α	Sector degree	23°
L_4	Anchor Length	30 μm
L_5	Stubs Length	580 μm
g_1	Gap spacing Between beam and transmission line in down state	0.15 μm
g_2	Gap spacing Between beam and transmission line in up state	2 μm

2.2. Pattern Reconfigurable Principles

The antenna can achieve reconfiguring by changing the current phase of adjacent elements. In this paper, the proposed antenna is designed by loading two microstrip MEMS switches. As shown in Fig. 1, the driven patch and each parasitic patch are equivalent to two radiating patches placed vertically. Whether the parasitic patch is driven by the excitation signal, it is controlled by MEMS switch. In Fig. 2, the antenna surface current distributions of four operating modes are shown. It is illustrated that when the MEMS switch is in the up state, the current intensity of the corresponding parasitic patch increases, leading to enhancing the radiation intensity. But when the switch is in down state, the current intensity of parasitic patches does not change significantly. So it is observed that the majority of the surface-current distributions in mode-1 and mode-2 are asymmetrical. In mode-1, the surface-current distribution is stronger on the left parasitic patch, but on the right one for mode-2. With the symmetrical switch configurations of both mode-3 and mode-4, their surface-current distributions are also symmetrical.

The driven patch and parasitic patch are placed vertically. As illustrated in Fig. 2, their radiation boundaries are also vertical; therefore, their radiation pattern should have a phase difference of 90°, firstly. At the same time, there is an initial excitation current phase difference for the driven patch and parasitic patch. Due to the presence of the phase difference between the driven patch and parasitic patch radiation patterns, the shift of total radiation pattern after super position will exists compared with conventional single patch antenna, and the angle of shift is related to the size of the phase difference. So the radiation pattern reconfigurable antenna can achieve by changing the state of MEMS, which affects the surface current distribution.

We can analyze the total radiated electric field including one driven element and one parasitic element as

$$E_{\text{total}}(r) = a_{\text{driven}} E_{\text{driven}}(r) + a_{\text{para}} E_{\text{para}}(r - r_0) \tag{1}$$

where r is the observation vector; r_0 is the distance vector between the driven element center and the parasitic element center; a_{driven} and a_{para} are the complex element excitation coefficients, E_{driven} and E_{para} are the electric fields radiated from the driven element and the parasitic element, respectively. In

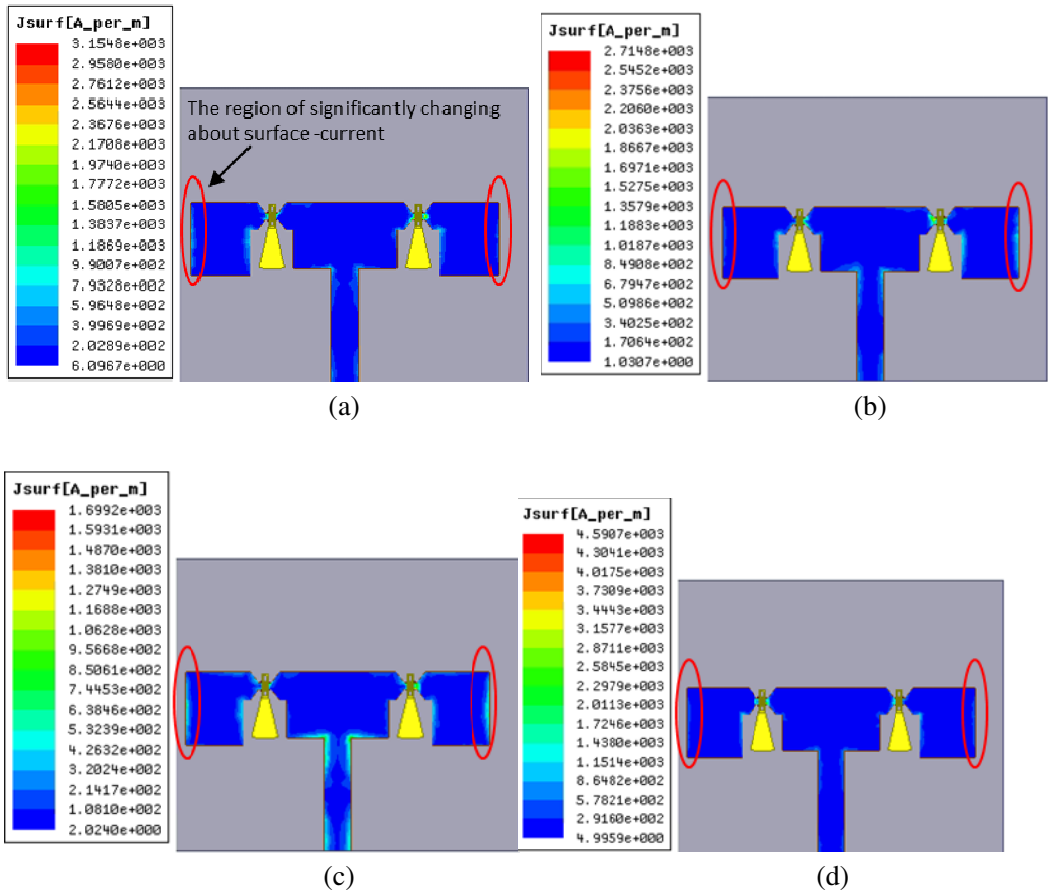

Figure 2. Surface-current distribution in (a) modes-1, $g_2 = 2\,\mu\text{m}$, $g_1 = 0.15\,\mu\text{m}$, (b) modes-2, $g_2 = 2\,\mu\text{m}$, $g_1 = 0.15\,\mu\text{m}$, (c) modes-3, $g_2 = 0.15\,\mu\text{m}$, $g_1 = 0.15\,\mu\text{m}$, (d) modes-4, $g_1 = 0.15\,\mu\text{m}$, $g_1 = 0.15\,\mu\text{m}$.

the far field, we can write the element pattern as

$$E_{\text{driven}}(r) = \frac{e^{-jkr}}{r} F(\theta, \phi) \tag{2}$$

$$E_{\text{para}}(r - r_0) = \frac{e^{-jk(r-r_0)}}{r} F\left(\theta, \phi + \frac{\pi}{2}\right) \tag{3}$$

where $F(\theta, \phi)$ is the far-field pattern distribution [14].

3. SIMULATED AND MEASURED RESULTS

In this paper, the return loss, gain, and the radiation pattern of the proposed antenna have been simulated and measured. The simulated results are illustrated in Table 2. The resonant frequency of four operating modes are basically the same, about 35.4 GHz. When the antenna works in modes-1 and modes-2, the radiation pattern will generate 14° phase shift, and the gains are 5.664 dB and 5.731 dB, respectively. But the maximum gain radiation angles of the proposed antenna are 0° for both modes-3 and modes-4. The gains are 5.801 dB and 5.856 dB, respectively. The simulation results of H-plane pattern are shown in Fig. 4 for the four modes. It is clear that the proposed antenna can achieve three radiation directions for four different modes.

The designed antenna size is too small, which results in that the actuation voltage is applied to MEMS switches difficultly, and it is difficult to test the antenna. So we designed a novel test scaffold. According to the results of simulation and optimization by software, the prototype antenna, shown in Fig. 5, was fabricated. Then the antenna performance was measured by a vector network analyzer

Table 2. Simulated data of the four modes of the antenna.

Mode No.	Switch_Left	Switch_right	frequency (GHz)	Angle (deg)	Gain (dB)
Mode-1	up	down	35.4	$-14°$	5.664
Mode-2	down	up	35.3	$14°$	5.731
Mode-3	down	down	35.3	$0°$	5.801
Mode-4	up	up	35.0	$0°$	5.856

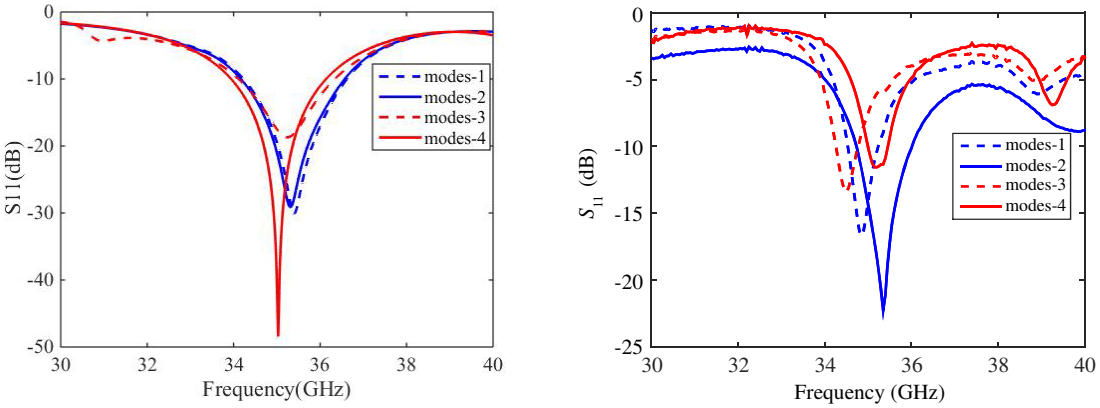

Figure 3. The return loss for different modes. (a) Simulation result, (b) measured result.

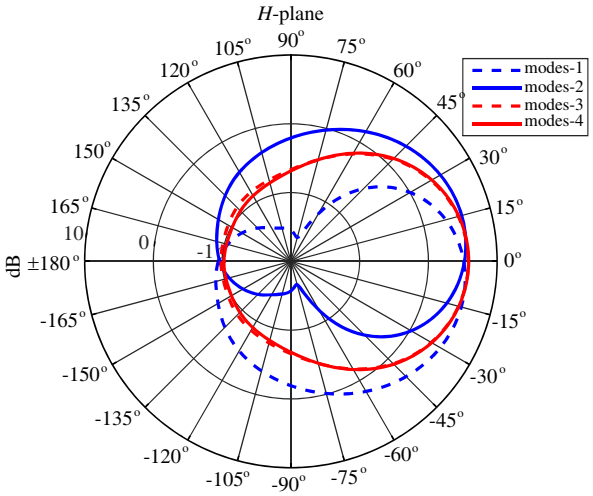

Figure 4. The simulation results of radiation pattern in H-plane for different modes.

(Agilent PNA N5442A Network Analyzer, the frequency range of 10 MHz–43.5 GHz) and the test system of far-field pattern. Fig. 3 shows the simulated and measured return losses of the proposed antenna for different modes. The measured resonant frequencies are 34.9 GHz, 35.4 GHz, 34.5 GHz, 35.2 GHz for the four modes, respectively. As can be seen from the plot, the measured results are closely consistent with the simulation results. The discrepancy can be observed at the return loss depth due to the SMA connector and test-scaffold not being included in the simulation.

Figure 6 shows the measured radiation patterns in the H-plane, and the measured maximum radiation directions and peak gains for the four modes. The maximum radiation directions of modes-1, modes-2, modes-3, modes-4 are $\theta = 17°$, $-25.8°$, $3.5°$, $0.7°$, respectively. The peak gains at the maximum radiation direction are 5.78 dBi, 6.49 dBi, 7.24 dBi, 6.31 dBi, respectively. The maximum

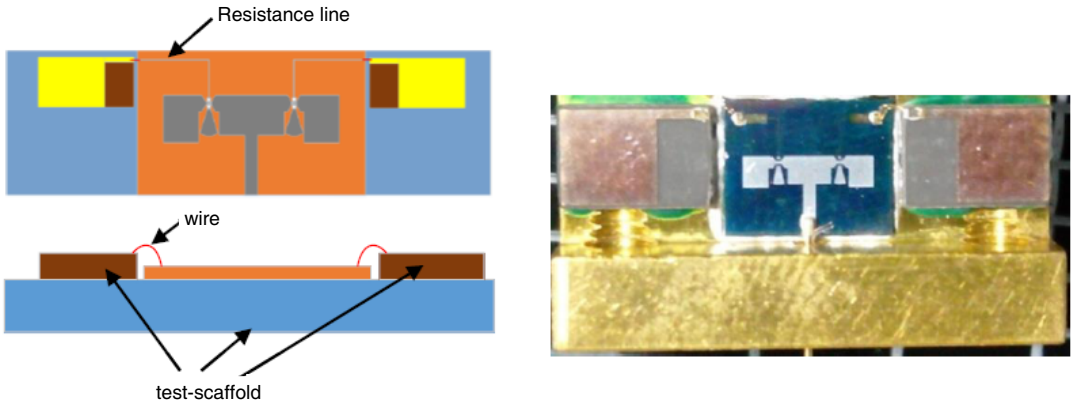

(a) (b)

Figure 5. Antenna structure diagram with test-scaffold. (a) Top view and side view, (b) fabricated antenna.

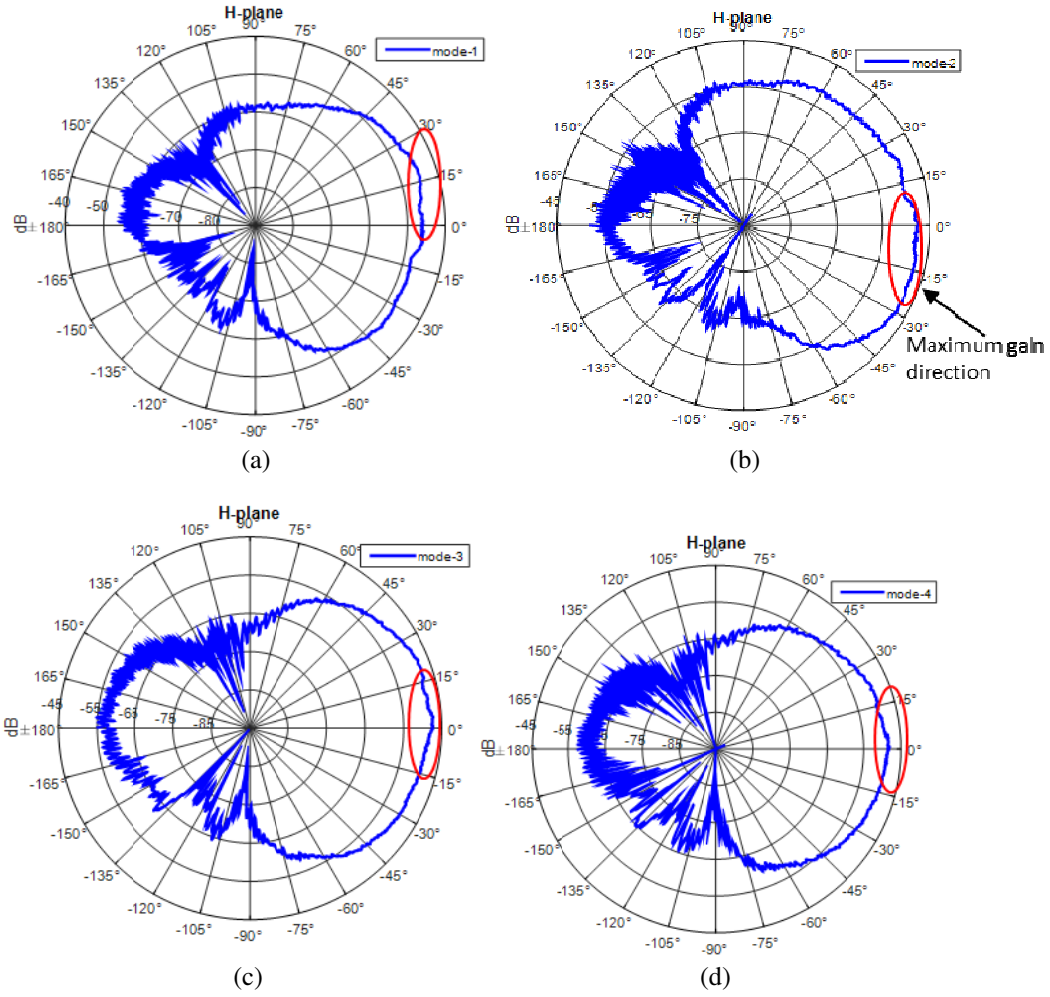

(a) (b)

(c) (d)

Figure 6. Measured radiation patterns of H-plane, (a) modes-1; (b) modes-2; (c) modes-3; (d) modes-4.

radiation gains achieve three beam directions for the four modes. But compared with simulated results in Table 2, the measured gains are a little bigger. It is mainly caused by reflection of test-scaffold because of excessive size. So both simulated and measured results demonstrate that the proposed antenna can realize radiation pattern reconfiguring by changing the states of MEMS switches.

4. CONCLUSION

This paper designs a pattern reconfigurable antenna, which integrates microstrip patch with MEMS switches. By controlling the switches between the driven patch and parasitic patches, the radiation pattern reconfigurable antenna can be realized. Due to its small size and light weight, the antenna has great potential for RF integrated circuits and for applying to satellite communication.

ACKNOWLEDGMENT

This work was supported by Program of National Science and Technology Support, under Grant No. 2014BAK12B00.

REFERENCES

1. Khidre, A., F. Yang, and A. Z. Elsherbeni, "A patch antenna with a varactor-loaded slot for reconfigurable dual-band operation," *IEEE Trans. Antennas Propag.*, Vol. 63, No. 2, 755–760, Feb. 2015.
2. Xiao, S., C. Zheng, M. Li, J. Xiong, and B.-Z. Wang, "Varactor-loaded pattern reconfigurable array for wide-angle scanning with low gain fluctuation," *IEEE Trans. Antennas Propag.*, Vol. 63, No. 5, 2364–2369, May 2015.
3. Jung, T. J., I.-J. Hyeon, C.-W. Baek, and S. Lim, "Circular/linear polarization reconfigurable antenna on simplified RF-MEMS packaging platform in K-band," *IEEE Trans. Antennas Propag.*, Vol. 60, No. 11, 5039–5045, Nov. 2012.
4. Qin, P.-Y., Y. J. Guo, A. R. Weily, and C.-H. Liang, "A pattern reconfigurable U-slot antenna and its applications in MIMO systems," *IEEE Trans. Antennas Propag.*, Vol. 60, No. 2, 516–528, Feb. 2012.
5. Cao, W., B. Zhang, A. Liu, T. Yu, D. Guo, and K. Pan, "A reconfigurable microstrip antenna with radiation pattern selectivity and polarization diversity," *IEEE Antennas Wireless Propag. Lett.*, Vol. 11, 453–456, 2012.
6. Van Caekenberghe, K. and K. Sarabandi, "A 2-bit ka-band RF MEMS frequency tunable slot antenna," *IEEE Antennas Wireless Propag. Lett.*, Vol. 7, 179–182, 2008.
7. Petit, L., L. Dussopt, and J.-M. Laheurte, "MEMS-switched parasitic-antenna array for radiation pattern diversity," *IEEE Trans. Antennas Propag.*, Vol. 54, No. 9, 2624–2631, Sep. 2006.
8. Zohur, A., H. Mopidevi, D. Rodrigo, M. Unlu, L. Jofre, and B. A. Cetiner, "RF MEMS reconfigurable two-band antenna," *IEEE Antennas Wireless Propag. Lett.*, Vol. 12, 72–75, 2013.
9. Rajagopalan, H., J. M. Kovitz, and Y. Rahmat-Samii, "MEMS reconfigurable optimized E-shaped patch antenna design for cognitive radio," *IEEE Trans. Antennas Propag.*, Vol. 62, No. 3, 1056–1063, Mar. 2014.
10. Kovitz, J. M., H. Rajagopalan, and Y. Rahmat-Samii, "Design and implementation of broadband MEMS RHCP/LHCP reconfigurable arrays using rotated E-shaped patch elements," *IEEE Trans. Antennas Propag.*, Vol. 63, No. 6, 2497–2507, Jun. 2015.
11. Chris, M., L. Gonzalez, and W. Hall, "Relative performance of mobile networks in the Ku, commercial Ka and government Ka bands," *Military Communications Conference*, 2081–2086, Baltimore, MD, Nov. 7–10, 2011.
12. Deng, Z. L., H. Gong, S. Fan, and C. H. Chen, "Ka-band radiation pattern reconfigurable microstrip patch antenna employing MEMS switches," *Applied Mechanics and Materials*, Vols. 411–414, 1674–1679, Sep. 2013.
13. Rebeiz, G. M., *RF MEMS: Theory, Design, and Technology*, Wiley, New York, 2003.
14. Balanis, C. A., *Antenna Theory Analysis and Design*, 3rd edition, Wiley, Hoboken, New Jersey, 2005.